Process Safety and Environmental Protection 170 (2023) 479–490

Contents lists available at ScienceDirect

Process Safety and Environmental Protection

journal homepage: www.journals.elsevier.com/process-safety-and-environmental-protection

Fully automated method to estimate opacity in stack and fugitive emissions: A case study in industrial environments

Oscar D. Pedrayes, Rubén Usamentiaga *, Daniel F. García

Department of Computer Science and Engineering, University of Oviedo, Campus de Viesques, Gijon 33204, Asturias, Spain

ARTICLE INFO

Keywords:
Deeplab
Deep learning
Pollution
Semantic segmentation
Smoke
2000 MSC:
0000
1111
PACS:
0000
1111

ABSTRACT

Fugitive emissions are those that are unplanned, i.e., they do not come out of a stack. These emissions are usually disperse and difficult to locate. By estimating the opacity of fugitive emissions they can be controlled or even prevented, helping to comply with environmental regulations. Most opacity estimation methods are based on stack emissions, which are straightforward, as they are always located in the same area. All methods in the literature for emission opacity estimation require a human operator to select the regions to be used as a reference. In this work, deep learning networks are proposed to improve the quality and automation of this process by selecting the regions completely and automatically. Furthermore, a new fugitive emission opacity estimation method is proposed. This method, called SBPB, is compared with other relevant methods in the literature, offering a solution with an average F1-Score metric 5 % higher than other methods on two real datasets with over 4000 images in total. This method provides a robust solution for fugitive emissions.

1. Introduction

A system capable of estimating the severity of an emission in real-time would be of great help in preserving the environment. Such a system could act in function of the severity of the emission, generating an alarm to solve the problem as quickly as possible. Moreover, it would comply with regulations that require industrial plants to monitor the severity of their emissions according to their size and opacity. To calculate the severity of an emission, one of the most important characteristics is opacity: the focus of this study.

Initially, emission plume opacity was assessed by visual comparison of the plume with Ringelmann charts (Ringelmann and Kudlich, 1967). These have five density reference levels inferred from a grid of black lines on a white surface, corresponding to different opacity values (Randolph and Foster, 1993). Later, the Method 9 standard (Randolph and Foster, 1993) was created to train human observers. Method 9 is a standard that details a method designed by the Environmental Protection Agency (EPA) of The United States to guide human observers in quantifying plume opacity in daylight conditions. Today, the most common way to obtain the opacity of a plume is still by human observers, usually trained with Method 9.

Standards and algorithms to determine the opacity of a plume do exist. ASTM D7520 () is a testing standard to determine the opacity of visible emissions using a digital camera and analysis software, known as Digital Camera Opacity Technique, or DCOT. ATSM D7520–09 was approved in 2009 by the U.S. Department of Defense (DOD). This standard aims to establish a minimum level of performance for products using DCOT to determine plume opacity outdoors. EPA Alternative Method 082 (ALT-082) is a standard (Dolan, 2017) approved in 2011 as an alternative to EPA Method 9 and adds limitations to the ASTM D7520 specification. The objective of ALT-082 is to determine the accuracy and reliability of a visual opacity monitoring system consisting of a conventional digital camera and a stand-alone software application to determine plume opacity. This standard was designed for the opacity analysis software Digital Opacity Compliance System (DOCS) (McFarland et al., 2004, 2007, 2010). There is also an updated version known as Digital Opacity Compliance System Second Generation (DOCS II) (Rasmussen and Grieco, 2009).

Some algorithms simulate the EPA Method 9 standard using two cameras. One of them is focused on the background taken as a reference and the other on the plume (Lighty et al., 2007). Other algorithms, such as the Digital Opacity Method (DOM) (Du et al., 2007), rely on a physical model of a reference background. In this case, DOM uses only one camera, so obtaining the reference is more complicated. If the reference is a contrasting background, it is called the Contrast model, while if the

* Corresponding author at: University of Oviedo Department of Computer Science and Engineering, Campus de Viesques, Gijón, 33204, Asturias, Spain.
E-mail address: rusamentiaga@uniovi.es (R. Usamentiaga).

https://doi.org/10.1016/j.psep.2022.12.023
Received 17 August 2022; Received in revised form 8 December 2022; Accepted 8 December 2022
Available online 9 December 2022

Nomenclature

ALT-082	EPA Alternative Method 082.
ASPP	Atrous Spatial Pyramid Pooling.
ATSM	American Society for Testing and Materials.
CNN	Convolutional Neural Network.
DCOT	Digital Camera Opacity Technique.
DOCS	Digital Opacity Compliance System.
DOD	Department of Defense.
DOM	Digital Optical Method.
EPA	Environmental Protection Agency.
FN	False Negative.
FP	False Positive.
GPU	Graphics Processing Unit.
HSV	Hue, Saturation, Value.
IoU	Intersection over Union.
P	Precision.
PCA	Principal Component Analysis.
R	Recall.
RGB	Red, Green, Blue.
SBPB	Sky and Building Percentiles in the Blue channel.
SGDM	Stochastic Gradient Descent with Momentum.
TN	True Negative.
TP	True Positive.

reference background is the sky itself, it is called the Transmission model. Using the Transmission model, Yuen et al. (Yuen et al., 2017) and Yuen et al. (Yuen et al., 2018) add new references to the sky reference: a reference to the background where the emission is dark, usually because of a building; a reference where the emission is lighter, the sky in the background; and a reference to the darker part in the background, the building itself.

In opacity estimation algorithms, a human operator usually selects the references by selecting boxes with the regions to be used. If these regions are obtained automatically, the whole process of opacity calculation can be automated. In (Prakasa, 2017), an algorithm for opacity calculation using regions obtained by k-nearest neighbors, and then revised by an operator, is proposed.

Opacity estimation algorithms are usually applied to plumes but not to more diffuse emissions. Fugitive emissions are emissions that are not generated by a stack, i.e., emissions that are not planned. For this reason, characterizing the severity of these emissions by calculating the opacity is essential before taking proportional actions. Fugitive emissions are commonly caused in industrial plants by failures in the production, processing, transmission, storage, and use of fuels. These emissions can severely pollute the environment, endanger the lives of people and animals in the area, and contribute to the greenhouse effect (Laconde, 2018). For example, carbon dioxide emissions have an impact approximately one order of magnitude less than methane emissions from the oil and gas industries (Solomon et al., 2007).

There is very little work in the literature on opacity estimation of fugitive emissions. DOCS has an algorithm for fugitive emissions which obtains an image before the emission occurs and an image while the emission exists to compare the two. Nevertheless, it requires a human operator to establish the references. This approach is not viable for a fully automated system, as it is impossible to know how long a fugitive emission may last. This results in images that may have excessively different light or weather conditions. The ideal method would be able to calculate the opacity of fugitive emissions from a single static image without the intervention of a human operator.

This paper compares different methods to estimate emission opacity and proposes a method, SBPB (Sky and Building Percentiles in the Blue channel), to determine fugitive emission opacity (Laconde, 2018). Unlike other methods, the proposed method is fully automated, so no human operator intervention is required. One of its major advantages is its robustness, enabling the use of uncalibrated cameras with self-adjusting exposure time. For input, a single image is needed, in which the opacity of each pixel is characterized separately. This approach provides more information about the emission than if only one numerical value were used to represent the opacity of the whole emission, which is especially important for fugitive emissions due to their non-uniform nature. For this purpose, a semantic segmentation model capable of obtaining the regions of fugitive emissions, buildings, and the sky is first trained. Then, the sky and building regions are used as a reference to calculate the opacity of fugitive emissions so that a particular opacity value characterizes each emission pixel. A value for the total emission can be obtained by selecting a percentile. This value is used to make a numerical as well as a visual comparison with other methods in the literature. To make fair comparisons between the different methods, the same mask obtained from the semantic segmentation network is used as the basis for pixel selection in all the methods.

2. Methods and materials

2.1. Datasets

The images used in this study were obtained from two different industrial plants through surveillance cameras. The images were taken on sunny days, partially cloudy days, and very cloudy days. There are no images of heavy fog or rainy days. All of the images were taken in the summertime between dawn and dusk. Night-time images are not included because, as the area is not artificially lit, it is impossible to see the emission after dusk. The images of the datasets were provided by the owner of the industrial plants. In order to maintain their anonymity, the regions of the images belonging to the facilities have been censored using a Gaussian blur and a stripe mask. This censorship applies only to the images shown in this paper, not those for training or use.

Experts from the companies' industrial plants use on-site visual analysis to classify opacity. Datasets from two plants, totalling 4287 images were classified into three levels of opacity: Low, Medium, and High. Of the 2150 images from the first plant, 1400 were Low, 597 Medium, and 153 High. Of the 2137 images from the second plant, 1294 were Low, 593 Medium, and 150 High. Example images can be seen in Fig. 1.

The channels of these images consist of the red, green, and blue (RGB) bands and have a resolution of 2048×1536 pixels or 1024×768 pixels. To meet the semantic segmentation network requirements, all images are scaled to a constant smaller size using one of the most common interpolation algorithms: Bicubic interpolation. This reduces their computational cost and required VRAM usage. The best size is 512×384 because it maintains its aspect ratio and keeps the highest manageable resolution.

The ground truth for semantic segmentation training has the following classes: building, vapour (water vapour from chimneys), cloud, fire, fugitive emission, and sky.

2.2. Processing pipeline

In this paper, a new processing pipeline is proposed to fully automate the opacity estimation process. In this pipeline the opacity estimation algorithm can be interchanged following a loosely coupled approach, so that the different opacity estimation methods can be easily compared.

Fig. 2 shows a diagram of the processing pipeline. In this pipeline, the image is fed to a semantic segmentation convolutional neural network which outputs a prediction mask with the location of the emission. This

(a) Low opacity. (b) High opacity. (c) High opacity with intense luminosity. (d) After dawn.

(e) Before dusk. (f) Cloudy and foggy. (g) Brown emission. (h) Black emission.

Fig. 1. Examples from the datasets.

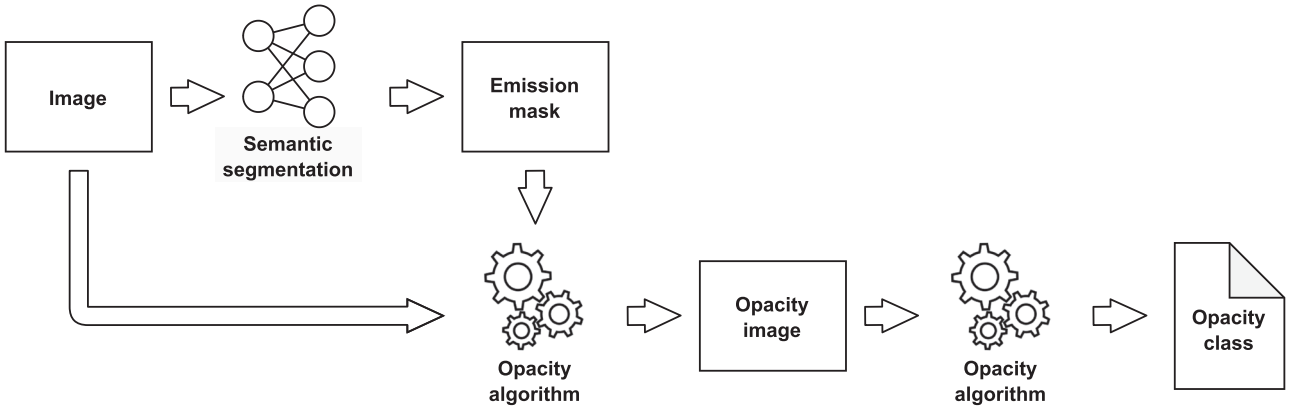

Fig. 2. Processing pipeline.

mask, along with the original image, is fed to the opacity estimation algorithm to calculate the opacity image, in which each pixel shows its opacity from 0 % to 100 %. Finally, this opacity image is used by a simple yet effective classification algorithm to determine the class of the emission opacity in order to calculate its metrics.

2.3. Semantic segmentation

Semantic segmentation networks are a type of convolutional neural network used for pixel classification. Pixel classification is useful to detect and localize objects or regions in images, which can be used to isolate the desired pixels. All convolutional neural networks must be trained before they can be used. To train a model, a groundtruth mask and the original image are needed. This groundtruth mask is necessary to calculate the errors made by the network and to correct them. Once the training process is completed, the prediction mask can be obtained when an image is fed to the network.

Convolutional neural networks have hyper-parameters to control their behavior during the training process. For this reason, in order to obtain optimal results, it is necessary to study the performance of the hyper-parameters. Since each modification in the hyper-parameters requires new training, this process can be extremely tedious and time consuming.

2.3.1. Network architecture

DeepLab (Chen et al., 2014, 2017a; Chen et al) is a convolutional neural network for semantic segmentation developed by Google. The latest version is called DeepLabv3 + (Chen et al., 2018). The architecture of the network combines an Atrous Spatial Pyramid Pooling (ASPP) module with a common encoder-decoder structure. In this paper, the official Tensorflow implementation from Google's Github[1] is used.

2.3.2. Metrics

All metrics are based on the concepts of true positive (TP), false positive (FP), true negative (TN) and false negative (FN). TP are pixels correctly classified as the target class, TN are pixels correctly classified as belonging to other classes, FP are pixels wrongly classified as the target class, and FN are pixels wrongly classified as belonging to other classes.

Precision is calculated as the percentage of correctly classified pixels from the total predicted pixels, as shown in Equation (1). Recall is

[1] https://github.com/tensorflow/models/tree/master/research/deeplab

Table 1
Training parameters for DeepLabV3+.

Training Parameters	
Input size	512 × 384 × 3
Classes	6
Backbone	Xception65
Output stride	16
Padding	Yes
Solver	Adam
Epochs	80
Batch size	6
Learning rate	0.00005
Class weighting	Median Frequency Weighting
Gradient clipping	No
L2 regularization	0.0004
Data augmentation	Scale 0.5–2.0 with 0.25 steps
Shuffle	Yes

calculated as the percentage of pixels classified correctly from the pixels that correspond to that particular class in the ground truth, as shown in Equation (2). If Precision is low and Recall is high, the predictions will overclassify pixels from that particular class. If Recall is low and Precision is high, only the pixels with high confidence will be classified as belonging to that particular class.

$$P = \frac{TP}{TP + FP} \tag{1}$$

$$R = \frac{TP}{TP + FN} \tag{2}$$

F_1-Score is one of the most common metrics in semantic segmentation. It is calculated as a combination of Precision and Recall as shown in Equation (3), and is equivalent to the Dice Coefficient with two classes.

$$F_1 = \frac{2 \times P \times R}{P + R} \tag{3}$$

Intersection-over-Union or IoU is equivalent to the Jaccard Index. This metric measures the area of similarity of a segmentation and its ground truth. It is calculated as the proportion between True Positives and the sum of True Positives, False Negatives, and False Positives, as shown in Equation (4),

$$IoU = \frac{Area\ of\ Overlap}{Area\ of\ Union} = \frac{TP}{TP + FN + FP} \tag{4}$$

2.3.3. Training

Before using the network, it must be trained. To obtain the best possible results, its hyper-parameters must be configured. Each time a hyper-parameter is modified, the network must be completely retrained to observe its effects on the results of its new model. As a starting point, to accelerate the convergence of the model, the training uses a pre-trained model[2] by Google on the Imagenet dataset (Deng et al., 2009)

Each hyper-parameter was adjusted individually because testing all possible combinations of hyper-parameters with a single computer would have been excessively time consuming. The final configuration used in this paper can be seen in Table 1. The GPU used to train the model was an NVIDIA RTX 2080 TI GPU with 11 GB of VRAM.

The following hyper-parameters were tuned: input sizes (2048 × 1536, 1024 × 768, 512 × 384, and 256 × 192); batch sizes; learning rate; epochs; output strides of 8, 16, and 32; different backbone networks (Resnet50, Xception45, Xception65, Xception71, MobileNetV2, MobileNetV3Small, MobileNetV3Large); L2 regularization; and solver algorithms (Adam or Stochastic Gradient Descent with Momentum (SGDM)).

To prevent overfitting, the dataset was shuffled to each epoch and data augmentation was used to obtain more training data. The augmentation process consisted of zooms of images with varying zoom values ranging from 50 % to 200 % at intervals of 25 % increments.

Pedrayes et al. (Pedrayes et al., 2022) provides additional information regarding the training process and its hyper-parameters for the datasets evaluated in this study.

Results of the test for the best model with data not seen by the network can be seen in Table 2. The F_1-Score for all classes is over 80 %, which gives high confidence in the prediction of the different regions. In particular, the Building, Vapour, and Sky classes are above 90 %. In Fig. 3 examples from all classes are shown. The first column shows the original image (with the building censored in red to maintain the anonymity of the company that provided the data), the second column shows the groundtruth, the third column shows the predictions, and the fourth and fifth columns show the groundtruth and the predictions overlaid on the original image. Almost all predictions are visually identical to the ground truth.

2.3.4. Regions

The sky pixels closest to the emission are used for those methods that require the sky reference to be obtained. For this purpose, the emission region is expanded and those pixels belonging to the sky class are selected. The number of sky pixels selected is equal to the number of emission pixels. Thus, emission and sky regions of the same size are obtained. For the process of selecting sky pixels, the pixels closest to the emission are discarded to avoid errors in the labeling of the regions. To do this, the fugitive emission mask is dilated once using a cross-shaped structure of 3×3 pixels. This value is used for both datasets, however, this gap can be increased depending on camera location, emission type

Table 2
Metrics of the best model test.

Class	Precision	Recall	IoU	F_1
Building	0.995	0.997	0.992	0.996
Vapour	0.915	0.900	0.831	0.907
Clouds	0.955	0.834	0.802	0.890
Fire	0.794	0.837	0.688	0.815
Emission	0.836	0.832	0.715	0.834
Sky	0.926	0.951	0.884	0.938

[2] https://github.com/tensorflow/models/blob/master/research/deeplab/g3doc/model_zoo.md

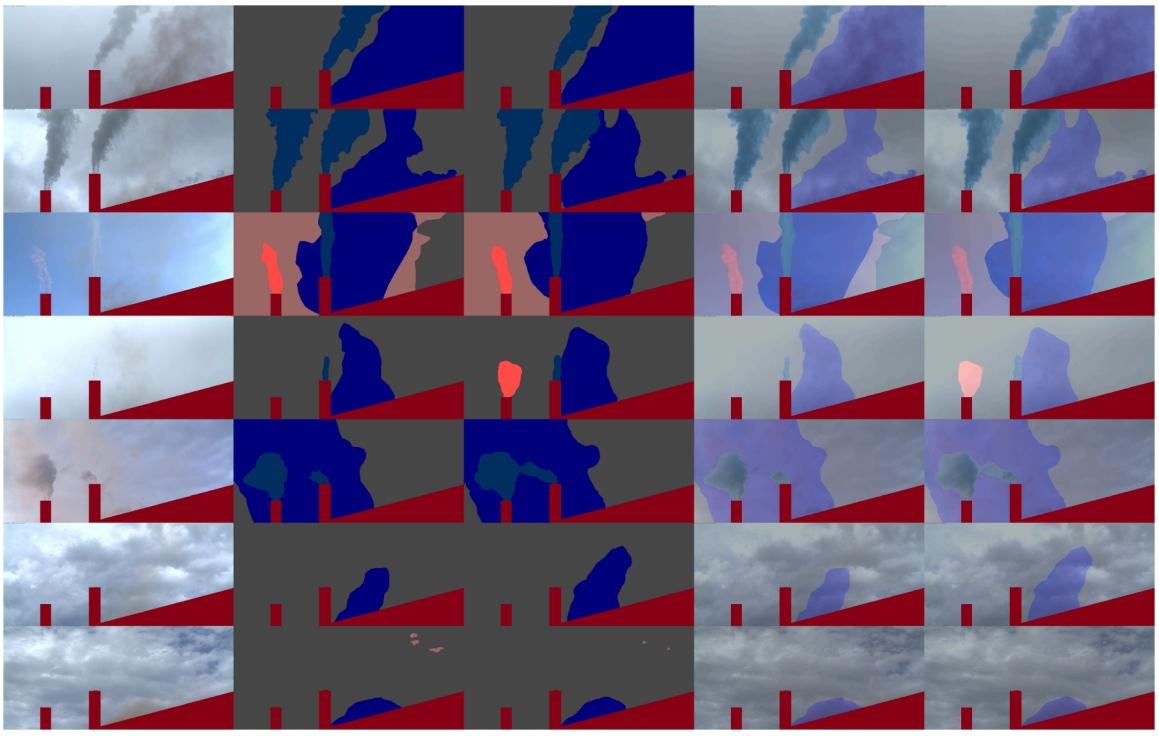

Fig. 3. Predictions (Building censored). Original image (1st column), ground truth (2nd column), prediction (3rd column), ground truth overlay (4th column), and prediction overlay (5th column).

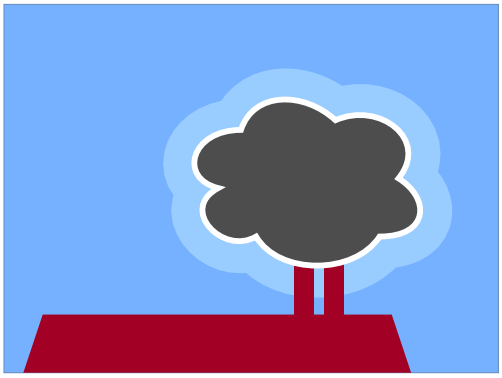

Fig. 4. Selection of the sky region.

Table 3
Opacity estimation methods.

Method	Citation	Type	Per pixel	Process
Ringelmann	(Ringelmann and Kudlich, 1967)	Stack	Yes	Manual
DOM (Transmission model)	(Du et al., 2007)	Stack	No	Manual
Prakasa et al.	(Prakasa, 2017)	Stack	Yes	Manual/ Assisted
Yuen et al.	(Yuen et al., 2017)	Stack	No	Manual
DOCS	(Rasmussen and Grieco, 2009)	Stack	Yes	Manual
Transmittance	(Randolph and Foster, 1993)	Stack	Yes	Manual
SBPB	Proposed	Stack/ Fugitive	Yes	Automatic

or accuracy of the model. Intuitively, it is clear that selecting the near-sky pixels rather than all sky pixels gives better results because of the comparison with the sky behind the emission, improving on operators that select arbitrary square bounding boxes.

A visual explanation can be seen in Fig. 4. The emission is shown in grey, the sky in dark blue, and the building in red. The white contour is the gap of the ignored sky pixels, and the light blue is the sky pixels used to calculate the opacity estimation.

2.4. Opacity estimation methods

This study evaluates all methods for opacity estimation in emissions published in the literature. The Ringelmann method is well-known in the literature, despite its age. The Prakasa et al. method is of little relevance in the literature but introduces an original approach. The DOM (Transmission Model), Yuen et al., and DOCS methods, on the other hand, are relatively recent and important in the literature. Finally, the Transmittance method is based on a well known equation. From the study of these methods, a new opacity estimation method called SBPB has been developed Table 3.

All methods in the literature are manual or, at most, assisted processes. In this paper an approach which allows the automatic use of any method thanks to the use of semantic segmentation is proposed. In order to make a fair comparison of all the methods, the extraction of regions from all of them is automated by means of semantic segmentation. This is due to the large number of images in the datasets, which makes manual testing impossible.

2.4.1. Method: ringelmann

The Ringelmann chart method is a rough adaptation of the first methodology based on a visual comparison with a chart. In this case, instead of a visual evaluation, the intensity of the emission converted to grayscale using the BT.709 recommendation (Series, 2017) is compared with the intensity of each chart reference (see Fig. 5a).

The pixel value 255 corresponds to 100 % luminous intensity, while 0 corresponds to 0 %. Fig. 5b shows the intensity values of the

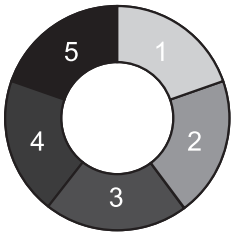

(a) Chart (Circle type).

Ringelmann scale	Light transmission (%)	Opacity (%)
0	[100,90)	[0,10]
1	[90,70)	(10,30]
2	[70,50)	(30,50]
3	[50,30)	(50,70]
4	[30,10)	(70,90]
5	[10,0]	(90,100]

(b) Intensity values per scale.

Fig. 5. Ringelmann method.

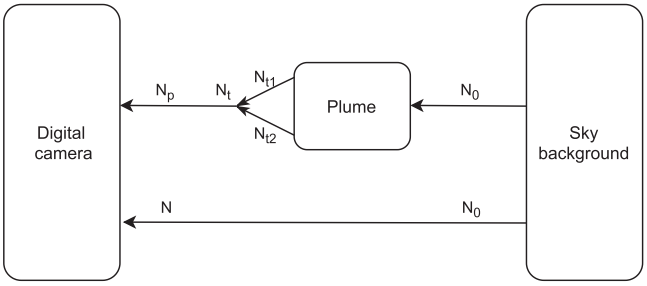

Fig. 6. DOM: Transmission model diagram.

Ringlemann scales. A major disadvantage of this method is that it is image-dependent, so two emissions with the same opacity level may differ depending on the scene lighting and camera calibration. This is because no reference is used to adjust the opacity calculation.

2.4.2. Method: DOM (Transmission model)

In the DOM (Transmission model) method, the opacity of the plume is determined by Equation (5). N_p refers to the value of the emission pixels. To calculate this value the average of all "emission" pixels is taken. N is the value of the background pixels. To calculate this value the average of all "sky" pixels is taken. K is a coefficient that depends on the transmissivity of the particles and the environment. According to (Du et al., 2007) and the DOM patent (Kim et al., 2009), a K value of 0.16 is recommended for black plumes and 1.4 for white plumes. This method is designed for uniform backgrounds. The dataset used contains dark emissions, thus a value of 0.16 is set for all images Fig. 6.

$$O = \frac{1 - \frac{N_p}{N}}{1 - K} \tag{5}$$

2.4.3. Method: Prakasa et al

The method described by (Prakasa, 2017) first divides the image into several rows containing the plume, so that each row will use reference values contained in the same row. This is done because it is assumed that the higher the elevation from the plume, the lower the emission density is. For this reason, the sky intensity values for a given row are averaged. Fig. 7 shows an example of a separation in rows.

Opacity is determined by comparing the color difference of the plume with the sky background and the maximum color difference. The maximum value is obtained by assuming that the color of the plume is pure black. Therefore, all values in the RGB channel will be zero to represent an all-black intensity. This maximum value can be considered as a reference to quantify the level of opacity.

Opacity is calculated for each pixel in the region individually. The intensities of neighboring pixels do not influence the calculation of the opacity of an observed point. Eqs. (6–8) are used to obtain the opacity value.

I_p is the value or intensity of the RGB band for the pixels belonging to the plume or emission. I_s are the pixels belonging to the linear fit representing the sky for the RGB bands.

$$d_{RGB} = \sqrt{(I_p - I_s)_R^2 + (I_p - I_s)_G^2 + (I_p - I_s)_B^2} \tag{6}$$

$$d_{Ref} = \sqrt{I_{p,R}^2 + I_{p,G}^2 + I_{p,B}^2} \tag{7}$$

$$O = \frac{d_{RGB}}{d_{Ref}} * 100\% \tag{8}$$

Equation (8) divides the value of the difference between the intensity of the emission pixel (I_p) and the intensity of the sky on the vertical axis of the region (I_s) by the intensity of the emission itself (I_p). This appears to be incorrect based on the physical equation for calculating opacity ($Opacity = 1 - I/I_0$, where I is the flux of light returning from the emission and I_0 is the flux of incident light without passing through the

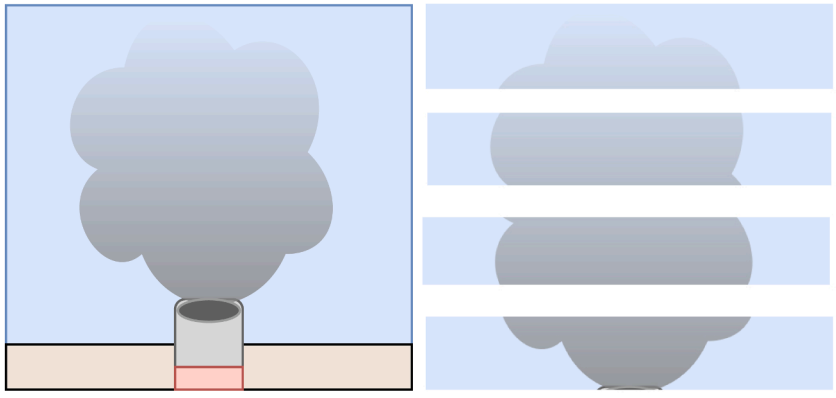

(a) Original image. (b) Division of the plume in several rows.

Fig. 7. Prakasa diagram.

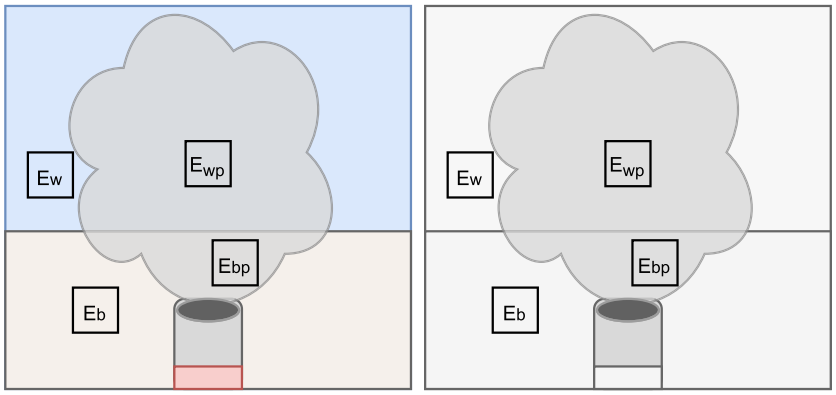

(a) Diagram of the Yuen et al. method. (b) Black and white image.

Fig. 8. Yuen et al.

emission), it should be divided by the intensity of the sky (I_s). The difference in intensities is normalized for each pixel separately. This normalization causes the opacity resulting from I_p values close to I_s to be minimized, while using values with a larger difference between I_p and I_s, the opacity value is maximized. It occurs because after dividing by I_p, when this is a very low intensity value, the value by which it is divided is also very low, and a division by 0 can occur if the I_p value is completely black. Similarly, when the two values are close, their difference, i.e. the numerator, will have a lower value. Also, in this case, the denominator will have a higher value, resulting in a much reduced opacity value. The major disadvantage of this method is that by visually representing a mask with opacity values, borders can be seen when dividing the image into regions. This method is not designed to create masks, but to obtain opacity plots along the vertical axis. However, masks are generated to provide a comparison with the rest of the methods.

2.4.4. Method: Yuen et al

The method described by (Yuen et al., 2017),(Yuen et al., 2018) splits the DOM (transmission model) method references according to the intensity of their background. The DOM (transmission model) uses only one reference for the sky and another for the emission. The Yuen et al. method uses two references for sky and two for emission. One of each pair of references is in a zone with higher intensity and the other in a zone with lower intensity. This method requires the BT.709 recommendation to convert RGB values to intensity values in a grayscale format.

This is done using Equation (9) where O is the opacity of the plume. E_{wp} is the amount of exposure caused by the bright background with plume. E_w is the amount of exposure caused by the bright background without plume. E_{bp} is the amount of exposure caused by the dark background with plume, and E_b is the amount of exposure caused by the dark background without plume. It can be understood visually, as shown in Fig. 8a.

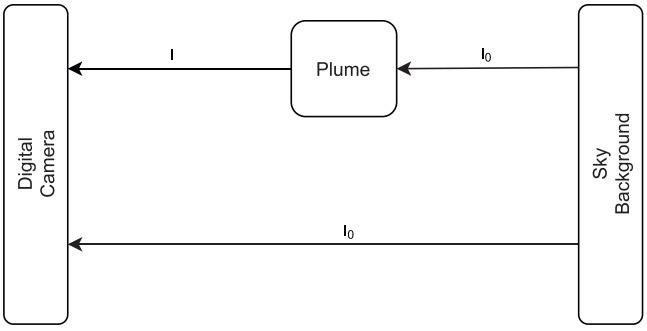

Fig. 9. Transmittance method diagram.

$$O = 1 - \frac{\frac{E_{wp}}{E_w} - \frac{E_{bp}}{E_w}}{1 - \frac{E_b}{E_w}} = 1 - \frac{E_{wp} - E_{bp}}{E_w - E_b} \tag{9}$$

2.4.5. Method: DOCS

For evaluation purposes, the DOCS method has been implemented in this work following its patent indications (Pfaff and Stretch, 2003). However, this version might not match the official implementation exactly because it leaves certain development aspects unexplained. In (Pfaff and Stretch, 2003; McFarland et al., 2004, 2010) it is explained that RGB is used for the whole process, although HSV can be used.

The first step of the DOCS method is to smooth out the image to eliminate or reduce visual artifacts (see (Pfaff and Stretch, 2003). The second step is to apply the PCA algorithm to the region of interest of the smoothed RGB image. This reduces the dimensionality of the data from three channels to one channel. The values obtained after using the PCA method represent the color intensity variability of the R, G and B bands. For this process only the first component of the PCA is used. For simplicity it will be called PCA1.

The third step is to calculate the opacity of the plume. The negative values of the PCA1 representation are directly related to the opacity through a linear relationship. In order to avoid images generating completely different results, this linear relationship is established on the complete dataset using a minimum and a maximum value. The minimum value is obtained by taking the 5th percentile of all the minima of each image in the dataset. The minima of each image is obtained using the 1st percentile to eliminate outliers. The maximum is obtained in the same way but using the 95th for the maxima and the 99th percentile to eliminate outliers.

2.4.6. Method: Transmittance

The Transmittance method is based on the transmittance formula (Randolph and Foster, 1993) shown in Eq. (10). As shown in Fig. 9, I is the intensity of the plume and I_0 the intensity of the sky. It is common for algorithms to follow a variation of this equation. For example, the transmittance method is similar to the DOM (Transmission model) method, but without the K value in this case. The purpose of the Transmittance method is to follow the physical model equation as simply as possible.

Intensity values are obtained using the BT.709 recommendation to transform the RGB image into intensity values in grayscale format. I_0 is calculated as the median of the sky region. The median is stronger than the average against outliers caused by reflective surfaces or possible artifacts in the image. I is the value of a particular pixel of the emission.

$$O = 1 - \frac{I}{I_0} \tag{10}$$

(a) Diagram of the original image. (b) Emission relative to the sky and building in the blue band. (c) Final result

Fig. 10. SBPB method diagrams.

2.4.7. Method: sky and building percentiles in the blue channel (SBPB) - proposed

In the methods described above, the emission must be black. With this method, the emission can be of others colors such as brown or yellowish, except blue (see Fig. 10a). Thus, because the sky/clouds generally have a blue hue, it is assumed that the more blue a pixel value is, the less opaque it is. Conversely, the lower its blue value, the more opaque. After some testing with the RGB bands separately and the grayscale using the BT.709 algorithm, all of them had trouble when sunlight was shining directly on the building. However, as the B-band is robust against this, it was decided to use only the B-band of the RGB images for opacity calculation.

This method establishes that the region segmented as Building has an opacity of 100 % and that the region segmented as Sky has an opacity of 0 %. To use this method, the building used as a reference cannot be blue (see Fig. 10b).

Based on this assumption, the 75th percentile value of the building region, and the 25th of the sky region is obtained. These percentiles provide robust reference values for the building and the sky, preventing outliers which may be caused by artifacts in the image or reflective surfaces (Vinutha et al., 2018). These intensity values can then be used to adjust the opacity calculation to the light conditions of the image. This enables the use of images obtained from dynamically self-adjusted or poorly calibrated cameras.

Given that the building has an opacity of 100 %, emission values equal to or lower than that of the building represent an opacity of 100 %. Those equal to or higher than the the sky region, have an opacity of 0 %. The remaining pixels, i.e., those between the two limit values, are normalized between 0 % and 100 % using these limit values, so that all emission pixels have values between 0 % and 100 % (see Fig. 10c).

3. Results and discussions

This section presents the most relevant examples for the comparison of the different methods. Figs. 11, 12, and 13 show the original image with the fugitive emission, and the results of the opacity estimation of the different methods in visual form where black is maximum opacity and white no opacity. Images with the opacity estimation show the values in the range [0,1] for each of the pixels.

Figure 11 shows that the proposed SBPB method is the only one which correctly classifies the opacity of the left central part of the emission. The Prakasa et al., DOCS, and Transmittance methods give that part of the emission an excessively low opacity level.

In situations with low intensity opacity (see Fig. 12), a larger difference between the methods is observed. This is caused by the higher complexity of the image due to lower contrast and higher confusion with the background clouds. The Ringelmann method values the pixels of the region by their intensity without taking into account the context of the image, causing these cases to estimate a higher opacity than expected. The DOM (Transmission model) method is not able to characterize the opacity of the emission. The Yuen et al. method overestimates the opacity in transition areas between emission and sky. The DOCS and Transmittance methods significantly improve the transition areas of the

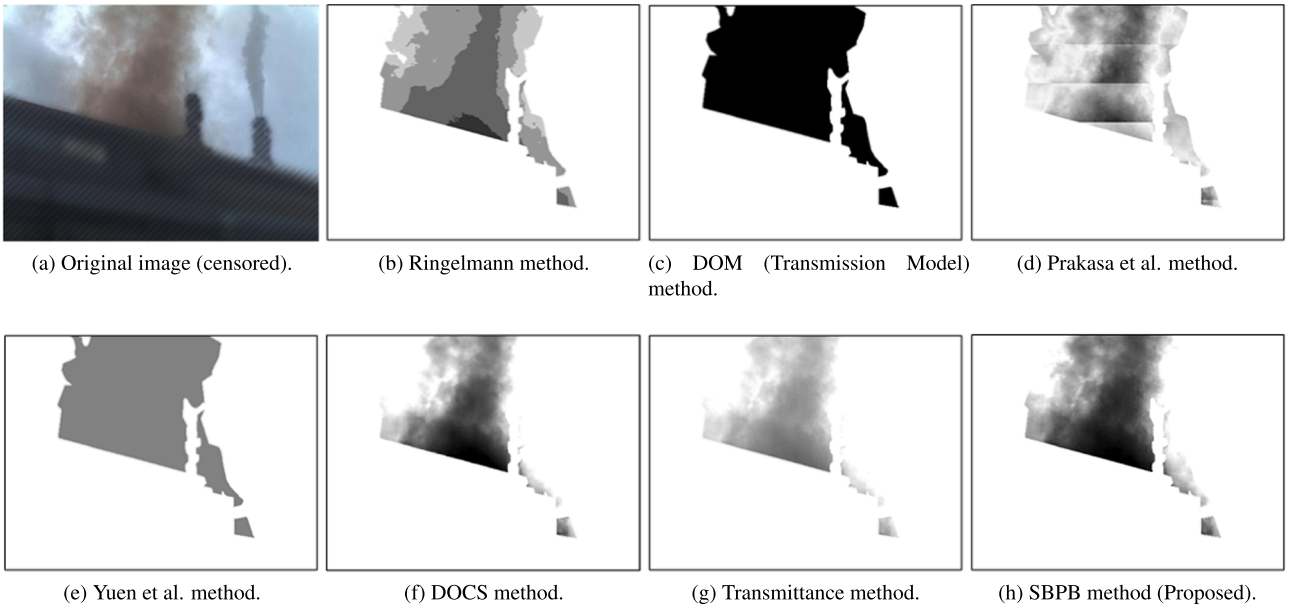

(a) Original image (censored). (b) Ringelmann method. (c) DOM (Transmission Model) method. (d) Prakasa et al. method.

(e) Yuen et al. method. (f) DOCS method. (g) Transmittance method. (h) SBPB method (Proposed).

Fig. 11. High opacity emission from the first dataset.

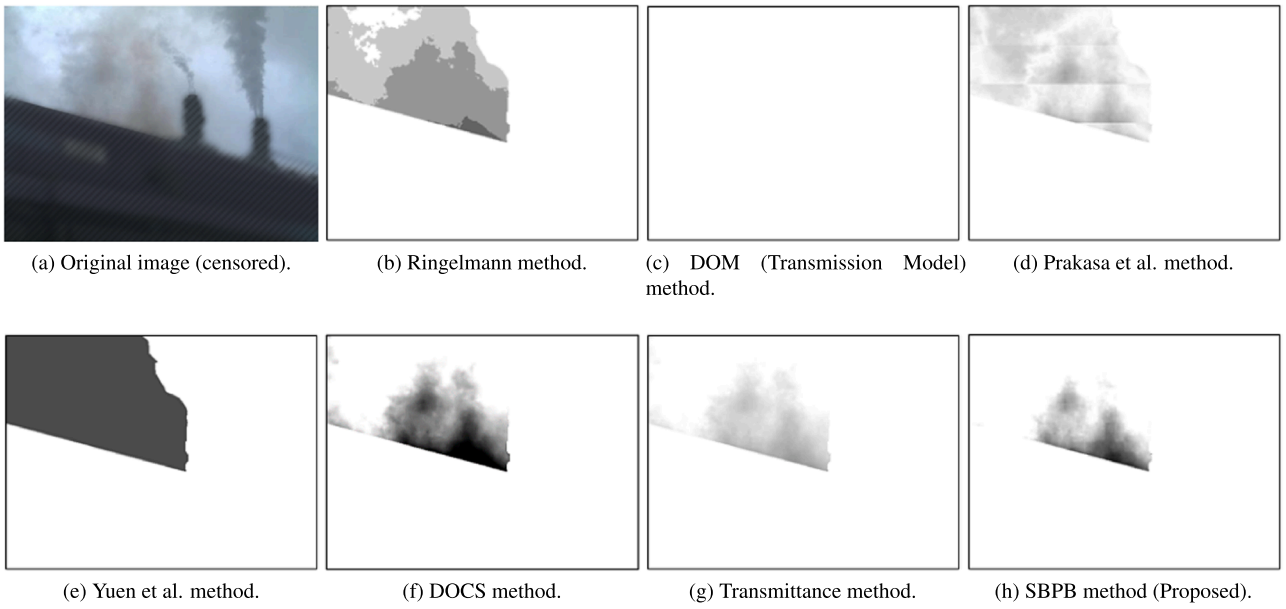

(a) Original image (censored). (b) Ringelmann method. (c) DOM (Transmission Model) method. (d) Prakasa et al. method.

(e) Yuen et al. method. (f) DOCS method. (g) Transmittance method. (h) SBPB method (Proposed).

Fig. 12. Low opacity emission from the first dataset.

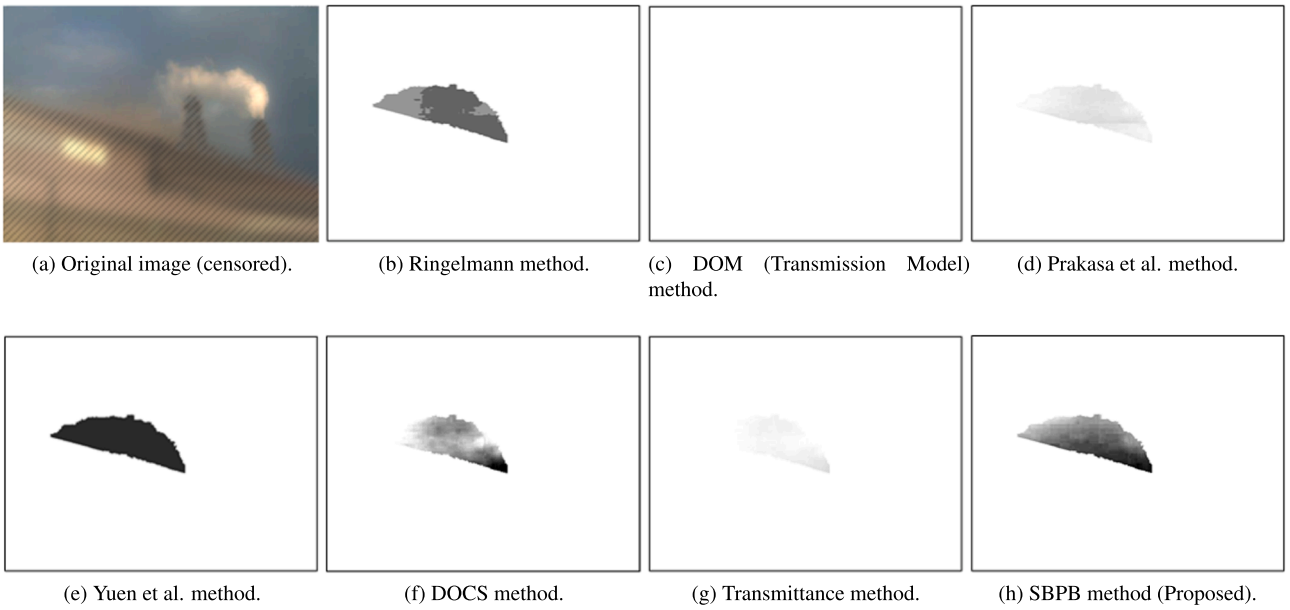

(a) Original image (censored). (b) Ringelmann method. (c) DOM (Transmission Model) method. (d) Prakasa et al. method.

(e) Yuen et al. method. (f) DOCS method. (g) Transmittance method. (h) SBPB method (Proposed).

Fig. 13. Intense luminosity opacity emission from the first dataset.

emission region, however, DOCS overestimates emission opacity. Finally, the proposed SBPB method further adjusts the emission region and provides opacity values closer to those expected.

Figure 13 shows that the DOM (Transmission model), Prakasa et al., and Transmittance methods are not able to determine the opacity of the emission correctly. In all these methods the emission is characterized at a very low opacity level. This is due to the fact that this image has a high light intensity, giving the building a high intensity. For this reason, the auto-tuning of the camera causes the sky to darken so that the sky is even darker than the building. However, the proposed SBPB method is able to characterize the emission opacity correctly. This is because, even though the luminous intensity is incorrect due to the camera autotuning, the sky still has a higher blue hue than the building. In this case, the Ringelmann method is not affected by the sky and the building, so it obtains its usual results. As the DOCS method is based on the variance of the image itself, it has fewer problems in characterizing the emission. Finally, the Yuen et al. method values the complete emission at the same time but is able to characterize this emission in a more reasonable way, which may be due to the use of multiple building and sky references.

Figure 14 shows the result of the opacity estimations of all methods for one of the images of the second dataset of another industrial plant. Here it can be seen that it performs similarly to the rest of the images of the first dataset. The main difference is that in this particular case the DOCS method seems to obtain similar results to the proposed SBPB method. These two methods are the ones that best estimate the opacity of the emission.

Methods that obtain a value for the whole emission, as is the case for DOM (Transmission model), and Yuen et al., are notably affected when the emission has very differentiated parts. That is, if half of the emission has a low opacity and the other half has a high opacity, the result is affected by obtaining an average value. If an operator selected a bounding box, the result would be completely dependent on where the

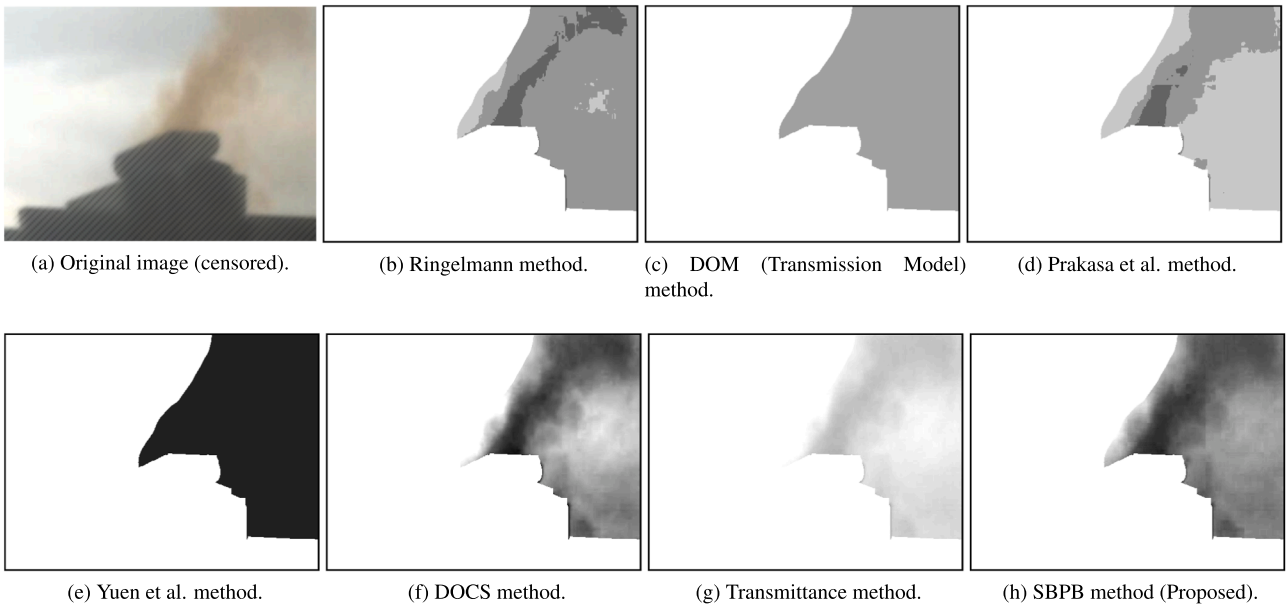

(a) Original image (censored). (b) Ringelmann method. (c) DOM (Transmission Model) method. (d) Prakasa et al. method.

(e) Yuen et al. method. (f) DOCS method. (g) Transmittance method. (h) SBPB method (Proposed).

Fig. 14. High opacity opacity emission from the second dataset.

Table 4
F_1-Score of the methods for the first dataset.

Method	Class			Average
	Low opacity	Medium opacity	High opacity	
Ringelmann	0.254	0.402	0.322	0.326
DOM (Transmission model)	0.663	0.336	0.415	0.471
Prakasa et al.	**0.804**	0.071	0.208	0.361
Yuen et al.	0.391	0.000	0.068	0.236
DOCS	0.586	0.019	0.125	0.243
Transmittance	0.747	0.413	0.478	0.546
SBPB (Proposed)	0.775	**0.456**	**0.540**	**0.590**

box were placed. For this reason, the automatic selection proposed in this work yields more reliable results despite the area weight of the different opacity levels. This is much more important for those methods in which the opacity is calculated for each pixel.

If the building has a higher light intensity than the sky, the methods that use the sky and the building as references may behave erroneously, as is the case for the DOM (Transmission model) and Yuen et al. methods. This is usually due to luminance situations which cause the camera autotuning to become very aggressive. In these cases, the proposed SBPB method achieves satisfactory results because the sky still has higher luminous intensity than the building in the B-band. Thus, the proposed method is much more robust in situations where the illumination is not perfect.

Table 5
F_1-Score of the methods for the second dataset.

Method	Class			Average
	Low opacity	Medium opacity	High opacity	
Ringelmann	0.609	0.000	0.185	0.264
DOM (Transmission model)	0.769	0.333	0.361	0.488
Prakasa et al.	**0.792**	0.224	0.000	0.339
Yuen et al.	0.554	0.000	0.107	0.230
DOCS	0.592	0.053	0.128	0.258
Transmittance	0.720	0.274	0.309	0.434
SBPB (Proposed)	0.753	**0.342**	**0.407**	**0.500**

In addition to the visual examples, Table 4 presents the information of the results of each method for the first dataset. Opacity images from the different opacity estimation algorithms are processed by a classification algorithm to obtain their categorical opacity level to be compared with the groundtruth generated by human operators. This classification algorithm discards opacity values lower than 5 % because they are the noisiest (Pfaff and Stretch, 2003), and calculates the 80th percentile of the remaining emission pixels to calculate a single opacity value for the whole emission. This is necessary because human visual perception of brightness is non-linear (McNamara et al., 2000). This single opacity value is used to determine its class (Low, Medium, or High) by using thresholds. These thresholds are calculated separately for each method in order to maximize the separation between classes for a fairer and more generalizable comparison. To calculate them, the midpoint between the median values of the adjacent classes is calculated. In other words, the threshold between the Low class and the Medium class is calculated as the sum of the median of the Low class with half the difference with respect to the Medium class. The threshold between the Medium and High class is calculated in the same way. The resulting classes are compared against a groundtruth to generate the F_1-Score metric seen in Table 4.

In view of the results shown in Table 4, it can be seen that the proposed SBPB method outperforms the other methods. This method has an average F_1-Score about 5 % better than the second best. Medium and High classes of the SBPB method have a much higher F_1-Score than the rest, however, the Prakasa et al. method outperforms the SBPB method in the Low opacity class. DOM (Transmission model) and Transmittance methods also produce a high Low opacity F_1-Score. The Prakasa et al., Yuen et al., and DOCS method have difficulty distinguishing between Medium and High opacity.

Table 5 shows the complete results of the second dataset. Here it can be seen that the results obtained are similar to those of the first dataset, maintaining the same conclusions. In this particular dataset, the Ringelmann method also struggles with the Medium and High opacity levels. This second analysis helps to validate the methodology and the robustness of the method.

3.1. Limitations

The SBPB opacity estimation method has several limitations that should be considered when using it. For example, the method is unable

to work at night, as it relies on the visibility of the emissions and the reference background. Other methods, such as DOM (Transmission model), can work at night, but they require the use of two cameras and two lights pointing towards the emission (Du et al., 2009). Additionally, the SBPB method is unable to work if the color of the building is blue or too bright, as this does not meet the requirement that the sky must have higher intensity in the blue band than the building. For this same reason, the emission intensity in the blue band must be darker than the sky and lighter than the building.

While these limitations may seem strict, most methods in the literature are based on the standard EPA Method 9, which has even stricter requirements. EPA Method 9 requires the observer to have a line of sight of about 18˚ when looking up to the emission, and the sun must be behind the observer, oriented in a 140˚ sector to the observer's back. This means that observations using EPA Method 9 can only be made at a particular time of the day, when the sun is in the correct position.

In contrast, the SBPB opacity estimation method allows for more flexibility in terms of the time of day and the conditions under which measurements can be taken. However, the method still requires a building and the sky as a reference in order to accurately compare the degree of opacity in the emissions. The accuracy of the method also depends on the accuracy of the semantic segmentation model used to identify and isolate the emissions. However, in the tested images, this accuracy was high, reaching about 90 % F1-Score. The method could be further improved with the use of better cameras, better lighting and weather conditions, and more spectral bands, such as infrared, to enhance the visibility and accuracy of the measurement. Overall, while the limitations of the SBPB opacity estimation method should be considered and more testing in different settings may be needed to fully validate the method, they are similar to those of other methods in the literature.

4. Conclusion

In this work, a method to estimate opacity of fugitive emissions capable of operating automatically without operator intervention is proposed. Existing methods for emission opacity estimation in images are not designed for fugitive emissions, and therefore have major limitations: these algorithms are always focused on black or white emissions, and they require an operator to select the regions to be used for the calculations.

While it is true that a large dataset is needed to train the network, the proposed method, SBPB, is the most stable of the methods presented due to its closeness to human operator assessments and its performance in different weather and lighting conditions such as a sunny or cloudy day at different times. This method can estimate opacity individually for each pixel, providing more information. One of its great advantages is that, thanks to the reference system, it does not require a properly calibrated camera without autotuning of exposure. A common camera such as a surveillance camera can be used. The use of semantic segmentation makes the SBPB method fully automatic i.e., it does not require the intervention of an operator. Furthermore, because this approach classifies all pixels in the image, more pixels can be employed as needed rather than a small section chosen by an operator. However, the greatest advantage of the SBPB method is its usefulness in characterizing fugitive emissions, since this task would be very difficult and time-consuming for a human operator. SBPB is capable of estimating the opacity of emissions of any color with low intensity in the B-band. The evaluated datasets contain brown and black emissions. Most methods are designed for pure black or pure white plumes. However, SBPB does not rely on a physical model that can be affected by a myriad of factors such as reflectivity indices and other variables, which may be different for each camera. Instead, it is based on a simpler idea: the assumption that the sky is blue, and that the building and emission are not blue. This simplicity makes it possible to extrapolate the method to various situations.

SBPB has an F_1-Score 4–7 % better than the Transmittance method, the second best performing method for Medium opacity. Furthermore, it also performs 6–10 % better than the Transmittance method, the second best performing method for High opacity. For Low opacity emissions, the SBPB method is outperformed by Prakasa et al. by about 3 %. However, the Prakasa et al. method tends to underestimate opacity which can be seen in its Medium and High opacity scores. The DOM (Transmission model) and Transmittance methods also produce similar Low opacity scores. The SBPB method is the most robust of all the discussed methods because it outperforms every other method for the Medium and High classes. This is confirmed when looking at the average of all three classes which surpass the second best method, Transmittance, by over 5–7 % for all classes.

Metrics and visual results indicate that SBPB can help monitor stack and fugitive emissions from industrial plants in real time even when using uncalibrated, self-adjusting exposure time monitoring cameras such as the ones used in this study. In this way, emissions can be monitored in realtime as they are detected, as well as recording the severity of emissions during the day. This would make it possible to penalize those industrial plants that do not respect current regulations, thus endangering the environment.

Declaration of Competing Interest

The authors declare that they have no known competing financial interests or personal relationships that could have appeared to influence the work reported in this paper.

Acknowledgments

This work has been partially funded by projects RTI2018-094849-B-I00 and PID2021-124383OB-I00 of the Spanish National Plan for Research, Development and Innovation.

Appendix A. Supporting information

Supplementary data associated with this article can be found in the online version at doi:10.1016/j.psep.2022.12.023.

References

Chen, L.-C., Papandreou, G., Kokkinos, I., Murphy, K., Yuille, A.L., 2017a. Deeplab: semantic image segmentation with deep convolutional nets, atrous convolution, and fully connected crfs. IEEE Trans. Pattern Anal. Mach. Intell. 40, 834–848.

L.-C. Chen, G. Papandreou, F. Schroff, H. Adam, Rethinking atrous convolution for semantic image segmentation, arXiv preprint arXiv:1706.05587 (2017b).

L.-C. Chen, G. Papandreou, I. Kokkinos, K. Murphy, A.L. Yuille, Semantic image segmentation with deep convolutional nets and fully connected crfs, arXiv preprint arXiv:1412.7062 (2014).

Chen, L.-C., Zhu, Y., Papandreou, G., Schroff, F., Adam, H., 2018. Encoder-decoder with atrous separable convolution for semantic image segmentation. ECCV 833–851 (pp.).

J. Deng, W. Dong, R. Socher, L.-J. Li, K. Li, L. Fei-Fei, Imagenet: A large-scale hierarchical image database, in: 2009 IEEE conference on computer vision and pattern recognition, Ieee, 2009, pp. 248–255.

Dolan, S.D., 2017. After considerable struggle, epa method 082 modernized visible emissions monitoring. Nat. Gas. Electr. 34, 21–25.

Du, K., Rood, M.J., Kim, B.J., Kemme, M.R., Franek, B., Mattison, K., 2007. Quantification of plume opacity by digital photography. Environ. Sci. Technol. 41, 928–935.

Du, K., Rood, M.J., Kim, B.J., Kemme, M.R., Franek, B., Mattison, K., 2009. Evaluation of digital optical method to determine plume opacity during nighttime. Environ. Sci. Technol. 43, 783–789.

B.J. Kim, M.J. Rood, K. Du, Digital optical method (dom™) and system for determining opacity, 2009.US Patent 7,495,767.

Laconde, T., 2018. Fugitive emissions: a blind spot in the fight against climate change. fugitives emissions-sector profile. INIS 51.

J.S. Lighty, K.E. Kelly, R.T. Whitaker, D.M. Weinstein, J. Desha, Enhancement of Digital Methods for Determination of Opacity, Technical Report, UTAH UNIV SALT LAKE CITY DEPT OF CHEMICAL ENGINEERING, 2007.

McFarland, M.J., Terry, S.H., Calidonna, M.J., Stone, D.A., Kerch, P.E., Rasmussen, S.L., 2004. Measuring visual opacity using digital imaging technology. J. Air Waste Manag. Assoc. 54, 296–306.

McFarland, M.J., Olivas, A.C., Atkins, S.G., Kennedy, R.L., Patel, K., 2007. Fugitive emissions opacity determination using the digital opacity compliance system (docs). J. Air Waste Manag. Assoc. 57, 1317–1325.
McFarland, M.J., Palmer, G.R., Olivas, A.C., 2010. Life cycle cost evaluation of the digital opacity compliance system. J. Environ. Manag. 91, 927–931.
McNamara, A., Chalmers, A., Troscianko, T., Gilchrist, I., 2000. Comparing real & synthetic scenes using human judgements of lightness. In: Eurographics Workshop on Rendering Techniques. Springer, pp. 207–218 (pp).
Pedrayes, O.D., Lema, D.G., Usamentiaga, R., García, D.F., 2022. Detection and localization of fugitive emissions in industrial plants using surveillance cameras. Comput. Ind. 142, 103731.
W.P. Pfaff, J. Stretch, Optical digital environment compliance system, 2003.US Patent 6,597,799.
E. Prakasa, et al., Development of imaging based method for plume opacity measurement, in: 2017 5th International Conference on Instrumentation, Control, and Automation (ICA), IEEE, 2017, pp. 212–216.
K. Randolph, K. Foster, Visible emissions field manual epa methods 9 and 22, U.S. Environmental Protection Agency (1993).
S. Rasmussen, P. Grieco, DOCS II as "ACE" in Lieu of an ASTM Standard for Digital Cameras, Technical Report, OGDEN AIR LOGISTICS CENTER HILL AFB UT AIR BASE WING (75TH), 2009.
Ringelmann, M., Kudlich, R., 1967. Ringelmann Smoke Chart. vol. 8333. US Bureau of Mines.
B. Series, Colour gamut conversion from recommendation itu-r bt. 2020 to recommendation itu-r bt. 709, International Telecommunication Union (2017).
Solomon, S., Manning, M., Marquis, M., Qin, D., et al., 2007. Climate change 2007-the physical science basis: Working group I contribution to the fourth assessment report of the IPCC. volume 4. Cambridge university press,.
Vinutha, H., Poornima, B., Sagar, B., 2018. Detection of outliers using interquartile range technique from intrusion dataset. In: Information and decision sciences. Springer, pp. 511–518 (pp).
Yuen, W., Gu, Y., Mao, Y., Koloutsou-Vakakis, S., Rood, M.J., Son, H.-K., Mattison, K., Franek, B., Du, K., et al., 2017. Performance and uncertainty in measuring atmospheric plume opacity using compact and smartphone digital still cameras. Aerosol Air Qual. Res. 17, 1281–1293.
Yuen, W., Gu, Y., Mao, Y., Kozak, P.M., Koloutsou-Vakakis, S., Son, H.-K., Mattison, K., Franek, B., Rood, M.J., 2018. Daytime atmospheric plume opacity measurement using a camcorder. Environ. Technol. Innov. 12, 43–54.